doi:10.1016/j.jmb.2007.01.035 J. Mol. Biol. (2007) 367, 1480–1493

JMB

Available online at www.sciencedirect.com

ScienceDirect

ELSEVIER

NMR Characterization of the Energy Landscape of SUMO-1 in the Native-state Ensemble

Ashutosh Kumar, Sudha Srivastava and Ramakrishna V. Hosur*

Department of Chemical Sciences, Tata Institute of Fundamental Research Homi Bhabha Road Mumbai 400 005, India

**Corresponding author*

Characterizing the low energy excited states in the energy landscape of a protein is one of the exciting and demanding problems in structural biology at the present time. These describe the adaptability of the protein structure to external perturbations. In this context, we used here non-linear dependence of amide proton chemical shifts on temperature to identify residues accessing alternative conformations in SUMO-1 in the native state as well as in the near-native states created by sub-denaturing concentrations of urea. The number of residues accessing alternative conformations increases and the profiles of curved temperature dependence also change with increasing urea concentration. In every case these alternative conformations lie within 2 kcal/mol from the ground state, and are separated from it by low energy barriers. The residues that access alternative conformations span the length of the protein chain but are located at particular regions on the protein structure. These include many of the loops, β2 and β5 strands, and some edges of the helices. We observed that some of the regions of the protein structure that exhibit such fluctuations coincide with the protein's binding surfaces with different substrate like GTPase effector domain (GED) of dynamin, SUMO binding motifs (SBM), E1 (activating enzyme, SAE1/SAE2) and E2 (conjugating enzyme, UBC9) enzymes of sumoylation machinery, reported earlier. We speculate that this would have significant implications for the binding of diversity of targets by SUMO-1 for the variety of functions it is involved in.

Keywords: energy landscape; SUMO-1; native-state ensemble; NMR

Introduction

Explicit description of the structure of the energy landscape of a given protein is the most desired, yet the most elusive topic in structural biology at the present time. The three-dimensional structure of a protein, determined either by X-ray crystallography or by NMR spectroscopy provides a picture of the native state of the protein at the bottom of the folding funnel. NMR relaxation measurements provide a measure of the dynamics at different locations in the protein structure in terms of the time scales and amplitudes of internal motions.[1,2] While these are extremely important characteristics that we need to know of the native state, it is also highly imperative to know in detail the shape and the energetic aspects of the funnel around the native state, since it is these features that dictate the structural adaptability, rates of inter-conversions between alternate conformations, perturbations to the energy landscape due to external agents such as ligands, substrates, inhibitors etc, or even due to changes in environmental conditions; these describe the dynamic energy landscape of the protein.[3,4] These in turn are crucial to understanding diversities in protein functions in a real system. However, such information has remained extremely difficult to obtain due to the absence of appropriate tools. NMR spectroscopic studies as a function of pressure over a wide range have been used in recent years to derive some information on the accessibility of alternate conformations by the different residues in a few proteins.[5–8] Pressure causes the protein to shrink, in some sense, thereby resulting in population of some low energy excited states. These show up as residue-wise chemical shift perturbations in a systematic manner.

Abbreviations used: HSQC, heteronuclear single quantum coherence; SUMO, small ubiquitin-related modifier; CD, circular dichroism.

E-mail address of the corresponding author: hosur@tifr.res.in

Alternatively, small temperature perturbations can also be used to populate alternative conformations accessed by individual residues in a given protein structure. These also will reflect in chemical shift perturbations of the individual residues. However, the states populated by temperature perturbations would of course be different from those populated by pressure perturbations. While it is still difficult to assess what these conformations are, some knowledge about their energy profiles relative to the most stable native state can be derived from an analysis of the chemical shift perturbations in either case. Williamson and co-workers[9–12] monitored the temperature dependence of the amide proton chemical shifts and observed that for any residue non-linearity of this dependence is an indication of the accessing of alternative conformations within a distance of 2–3 kcal/mol from the native state. Protein accesses these low-lying states for at least 1% of its time. Identification of such states under mild external perturbation, such as urea, will help in elucidating how the energy landscape of the protein can alter due to small external perturbations. Here, we have used this approach to characterize the energy landscape of SUMO-1 in the native state ensemble.

SUMO-1 (small ubiquitin related modifier), an important protein involved in post-translational modification, is a 101 amino acid residue polypeptide, which reversibly gets conjugated to many of the target proteins by a process called "sumoylation". Prior to sumoylation the protein gets activated by cleaving off four residues from the C-terminal end. Sumoylation proceeds *via* concerted action of activating enzyme (E1), conjugating enzyme (E2) and ligating enzyme (E3). E1 and E2 are the same in all sumoylation reactions but E3, the ligating enzyme, varies from substrate to substrate. E3-SUMO complexes recognize the substrates and then SUMO gets attached to the substrate *via* isopeptide bond formed between the carboxyl terminus of the G97 residue and a lysine in the substrate.[13,14] Post-translational modification by SUMO and its consequences in signaling is currently one of the major areas of research. Four examples of functional modulation in target proteins after SUMO modification are known till date.[13] SUMO modification can be in competition with ubiquitination and can alter the stability of the target protein. In recent years sumoylation has emerged as a regulator of diverse functions like signal transduction, transcription, chromatin remodelling, DNA repair, viral infection and nucleocytoplasmic shuttling.[15–17] Sumoylation has also been shown to play an important role in the neurodegenerative Huntington's disease.[18] Now, SUMO-1 is also believed to be involved in many non-covalent interactions as a potential regulatory mechanism in signal transduction pathways. Recent reports say that SUMO works as a "molecular glue" to facilitate the assembly of multiprotein complexes.[19–21] It has been suggested that SUMO-1 binds to parkin, an E3 ubiquitin ligase, and this association modulates the intracellular localization and self-ubiquitination of parkin.[22] We believe that SUMO-1 is able to perform these many diverse functions because of its dynamic structure and adaptability in the native state. Previous structural studies on SUMO-1 suggested that more than 50% of the protein is actually unstructured.[23–25] We have also shown that the flexible part of the protein is an important site for substrate binding.[25] Equilibrium folding studies on SUMO-1 indicated that the protein goes through an unusual sequence of transitions involving interesting structure forming and breaking processes as the protein folds from the unfolded state to the native state.[26] Here, we demonstrate by studying curved temperature dependence of amide proton chemical shifts, that a large number of residues in SUMO-1 (1–97) access alternative conformations; hereafter for sake of brevity we refer to this protein as SUMO-1 only. These low lying conformers are within 1–2 kcal/mol from the native state. We further elucidate the changes in the landscape of the protein at residue level in the presence of sub-denaturing concentrations of urea.

Results

Thermal denaturation from CD

We monitored the thermal unfolding of SUMO-1 by measuring ellipticity at 222 nm as a function of temperature as shown in Figure 1(a). Thermal denaturation is fully reversible with a transition mid-point (T_m) at 334.64(±0.08) K (61.64 °C) and shows a sigmoidal behavior. Sigmoidal behavior is generally shown by proteins that unfold/fold in cooperative manner illustrating a sharp transition from a specific tertiary structure to a denatured state. Equations (4) and (5) (see Materials and Methods) were used to derive the equilibrium constant ($K_{T(app)}$) and the free energy changes (ΔG_T^0) as a function of temperature. The fitting of ΔG_T^0 *versus* T data to equation (9) (Figure 1(b)) in the temperature range of the transition yielded the values of ΔC_P and ΔH_m. From this ΔH_m the value of ΔS_m was calculated as $\Delta H_m/T_m$. All the parameters so derived are summarized in Table 1. Then, using equation (9), the free energy difference between the native state and the thermally denatured state was calculated to be ~6.5 kcal/mol.

Temperature dependence of amide proton chemical shifts: theoretical simulations

Temperature dependence of amide proton chemical shifts in globular proteins has been investigated for more than three decades by many researchers and continues to be investigated even today.[9,27–33] The amide proton chemical shifts are directly proportional to bond magnetic anisotropy (σ^{ani}) and this is crucially dependent on H-bonding, either intramolecular or intermolecular. In the former case, the carbonyl groups, the H-bond acceptors play a

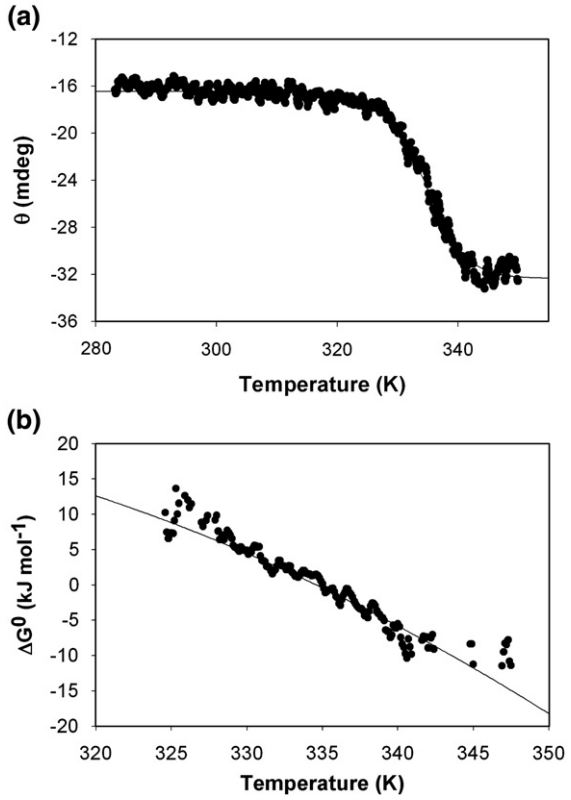

Figure 1. Thermal denaturation curve for SUMO-1 (pH 5.6) monitored by far-UV CD at 222 nm. Data are normalized as described in Materials and Methods. (b) Stability curve of SUMO-1 obtained by fitting the data in the transition region according to equation (9).

crucial role. The bond magnetic anisotropy (σ^{ani}) is proportional to r^{-3} where r is the distance between the affected amide proton and the centre of the bond magnetic anisotropy, which lies close to the oxygen atom in the carbonyl groups. In the case of solvent accessible groups, H-bonding with solvent molecules influences the amide proton chemical shifts. Thus, the amide proton chemical shift is critically dependent on the length of the H-bond that the proton is engaged in. The chemical shift of an amide proton is also intimately related to the local environment around it, especially the aromatic residues.

When the temperature of the solution is raised, thermal fluctuations increase, which results in an increase in the average distance between atoms; X-ray crystallographic studies at several temperatures (98–320 K) on ribonuclease-A indicated that the protein volume increases linearly with temperature to an extent of about 0.4% per 100 K.[34] Such an increase in the distance between the atoms participating in an H-bond results in a weakening of the H-bond. Consequently, chemical shifts of most amide protons move upfield when the temperature is increased. Since bond magnetic anisotropy (σ^{ani}) is proportional to r^{-3} and molecular volume (V) is proportional to r^3 ((σ^{ani}) α $1/V$), there is an inverse relationship of their variation with temperature. However, over a small temperature range, σ^{ani} may appear to decrease linearly with temperature, and consequently amide proton chemical shifts would appear to vary linearly with temperature. In BPTI and lysozyme, which are known to be extremely stable under a variety of extreme conditions, including temperature, it was indeed observed that the amide proton chemical shifts change linearly with temperature over the ranges, 279–359 K for BPTI and 278–328 K for lysozyme.[9] Such measurements have been carried out on many other proteins[28,35] and the temperature coefficients or the gradients of temperature dependence of the amide protons have been found to span a wide range, −16 to+ 4 ppb/K. For a strongly H-bonded amide this value is more positive than −4.5 ppb/K.[9] This is because the lengthening of the average H-bond distance will be greater for the intermolecular H-bond, such as those with bulk water, than for the intramolecular H-bonds.

However, if the protein structure is not very rigid, as would be the case for many systems, the chemical shifts would also be influenced by local structural and dynamics changes, and then the temperature dependence of chemical shifts may deviate from linearity. Indeed, in certain situations the amide proton chemical shifts have been seen to be non-linearly dependent on temperature, and this has been interpreted to indicate existence of alternate conformations that the residues can access.[12] A theoretical description and simulation in the temperature range 288–309 K, relevant to our present experiments on SUMO-1 are presented below.

Consider a residue having two conformational states accessible to it, i.e. a native state and a higher energy state. This high energy state could be either due to local conformational change along the backbone or due to changes in the surrounding side-chain packing. Of course, both of these effects can influence each other. Each of the two states can be assumed to have a linear chemical shift temperature dependence as, $\delta_1 = \delta^{\circ}_1 + g_1 T$ and $\delta_2 = \delta^{\circ}_2 + g_2 T$, where g_1 and g_2 are the gradients of temperature dependence, δ_1 and δ_2 are the chemical shifts of the native and excited states, respectively, and T is the temperature. If P_1, and P_2 are the corresponding populations of the native and the excited states, the

Table 1. Thermodynamic parameters from the analysis of thermal denaturation profile of SUMO-1 at 27 °C, pH 5.6, monitored by far UV-CD

	ΔH_m (kcal mol^{-1})	ΔS_m (kcal mol^{-1} K^{-1})	T_m (K)	ΔC_p (kcal mol^{-1} K^{-1})
Stability curve ΔG^0_T *versus* T (equation (9))	81.61±1.45	0.24	334.64±0.08	1.71±0.14

observed chemical shift, δ_{obs}, of the amide proton will be given by:

$$\delta_{obs} = \delta_1 P_1 + \delta_2 P_2 \quad (1)$$

These populations depend on the free energy difference between the two states. If there are more states contributing, then the observed shift will be a weighted average over all the accessible states. It is this complex dependence of chemical shifts on many thermodynamic and other factors that leads to non-linear dependence of chemical shifts on temperature. To understand the influence of these factors we performed simulations of H^N chemical shift variation with temperature in the range, 288 K–309 K, using a two state model following the procedure described:[12]

$$\delta_{obs} = \frac{(\delta_1^0 + g_1 T) + [(\delta_2^0 + g_2 T)e^{-(\Delta G/RT)}]}{1 + e^{-(\Delta G/RT)}} \quad (2)$$

where, ΔG is the free-energy difference between the two states and $\Delta G = \Delta H - T\Delta S$, where, ΔH and ΔS are the enthalpy and entropy differences between the two states, respectively.

The δ_{obs} obtained using the above equation was best fitted to a linear equation and the residuals were plotted against temperature to generate a profile of the deviations. The results are summarized in Figure 2. Figure 2(a) shows the curves for ΔG variation, ranging from 1–4 kcal/mol, with δ_1, δ_2, g_1 and g_2 being kept constant. It is interesting to note that the curvature almost disappears for $\Delta G \geq 3$ kcal/mol in the given temperature range. If the chemical shift of the ground state is upfield to that of the excited state, the shape of the curve changes from convex to concave as shown in the Figure. The smaller the ΔG, the larger is the curvature. Figure 2(b) illustrates the dependence of curvature on chemical shift differences for constant ΔG (for these, ΔG was chosen to be 2 kcal/mol). Figure 2(c) shows the effect of gradients on the curvature, when ΔG and chemical shifts are kept constant; here again ΔG was chosen to be 2 kcal/mol. It is clear that in either case (Figure 2(b) and (c)) the change in the curvature is very small. Thus, ΔG appears to be the most decisive parameter in defining the extent of the curvature. We also observed that for a constant ΔG, variation in ΔS (entropy) can cause a small change in the curvature (data not shown). Similarly, when the curvature is small due to some chosen value of ΔG, small variations in chemical shifts and gradients can make the curvature appear non-existent (data not shown). Therefore, a linear

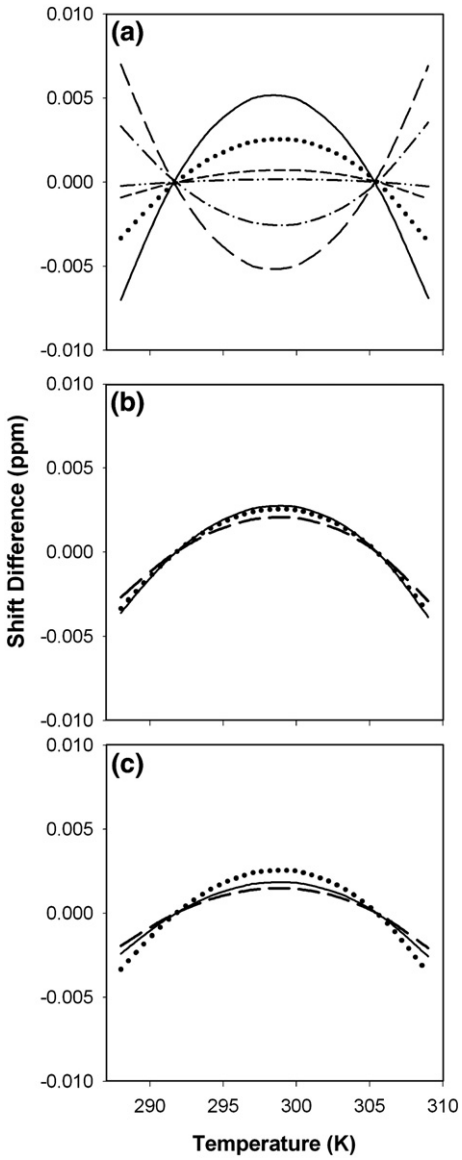

Figure 2. Simulation of dependence of H^N chemical shift variation with temperature in the range 288–309 K. In the entire set of calculations chemical shift was simulated using equation (2) given in the text and fitted to a straight line with temperature. The residuals (deviation from linearity) thus obtained were used to show the curvatures. (a) Different curves show the dependence of curvature on free energy difference between the native state and the alternate states. Convex shapes: $\Delta G = 1$ kcal/mol (continuous line), $\Delta G = 2$kcal/mol (dotted line), $\Delta G = 3$ kcal/mol (broken line), $\Delta G = 4$ kcal/mol (dot-dot-dashed). Concave shapes: $\Delta G = 1$ kcal/mol (long dashed line) and $\Delta G = 2$ kcal/mol (dot-dash line). For these calculations $T\Delta S$ was fixed to 5.1 kcal/mol at 298 K and ΔH was varied from 6.1 kcal/mol to 9.1 kcal/mol. The chemical shifts and gradients were: $\delta_1 = 8.8$ ppm, $\delta_2 = 8.0$ ppm, $g_1 = -2$ ppb/K and $g_2 = -7$ ppb/K for the convex shapes and $\delta_1 = 8.0$ ppm, $\delta_2 = 8.8$ ppm, $g_1 = -7$ ppb/K and $g_2 = -2$ ppb/K for the concave profile. (b) The effect of variation in the chemical shifts (δ_1 and δ_2) on curvature: Dotted curve shows the curvature for free energy difference of 2 kcal/mol with the other parameters same as in (a); continuous curve, $\delta_1 = 9.0$ ppm, $\delta_2 = 8.0$ ppm $g_1 = -2$ ppb/K and $g_2 = -7$ ppb/K and $\Delta G = 2$ kcal; broken curve, $\delta_1 = 8.3$ ppm, $\delta_2 = 8.0$ ppm, $g_1 = -2$ ppb/K and $g_2 = -7$ ppb/K and $\Delta G = 2$ kcal. (c) The effect of variation in the temperature gradients (g_1 and g_2) on the curvature: Dotted curve is the same as in (a) with $\Delta G = 2$ kcal/mol; continuous curve, $\delta_1 = 8.8$ ppm, $\delta_2 = 8.0$ ppm, $g_1 = -4$ ppb/K and $g_2 = -7$ ppb/K and $\Delta G = 2$ kcal; broken curve, $\delta_1 = 8.8$ ppm, $\delta_2 = 8.0$ ppm, $g_1 = -2$ ppb/K and $g_2 = -4$ ppb/K and $\Delta G = 2$ kcal.

dependence of amide proton chemical shifts on temperature puts only some limits on ΔG values and does not necessarily indicate absence of alternative conformations that the protein can access.

Temperature dependences in SUMO-1 in the native and near-native states

In a previous article, we observed that SUMO-1 unfolds *via* a complex pathway when subjected to urea denaturation.[26] There are two transitions with mid points 2.42 and 5.69 M. Therefore, to investigate the temperature dependences in the near-native states created by low concentrations of urea, we restricted the maximum concentration of urea to 0.9 M, which is much lower than the first transition mid-point (2.42 M) and the protein is ensured to remain in the native state ensemble.

We have measured the temperature dependence of amide proton chemical shifts in SUMO-1 by recording ^{15}N-^{1}H heteronuclear single quantum correlation (HSQC) spectra as a function of temperature in the range, 288–309 K, and at urea concentrations of 0, 0.35, 0.7 and 0.9 M. The folding-unfolding transition mid-point (T_m) for SUMO-1 has been determined to be 334.64 K (Figure 1), and thus in the above temperature range the protein is clearly in the native state ensemble. In the presence of the above concentrations of urea the transition mid-point is reduced marginally by only few degrees (3 °C at 0.9 M urea) (data not shown).

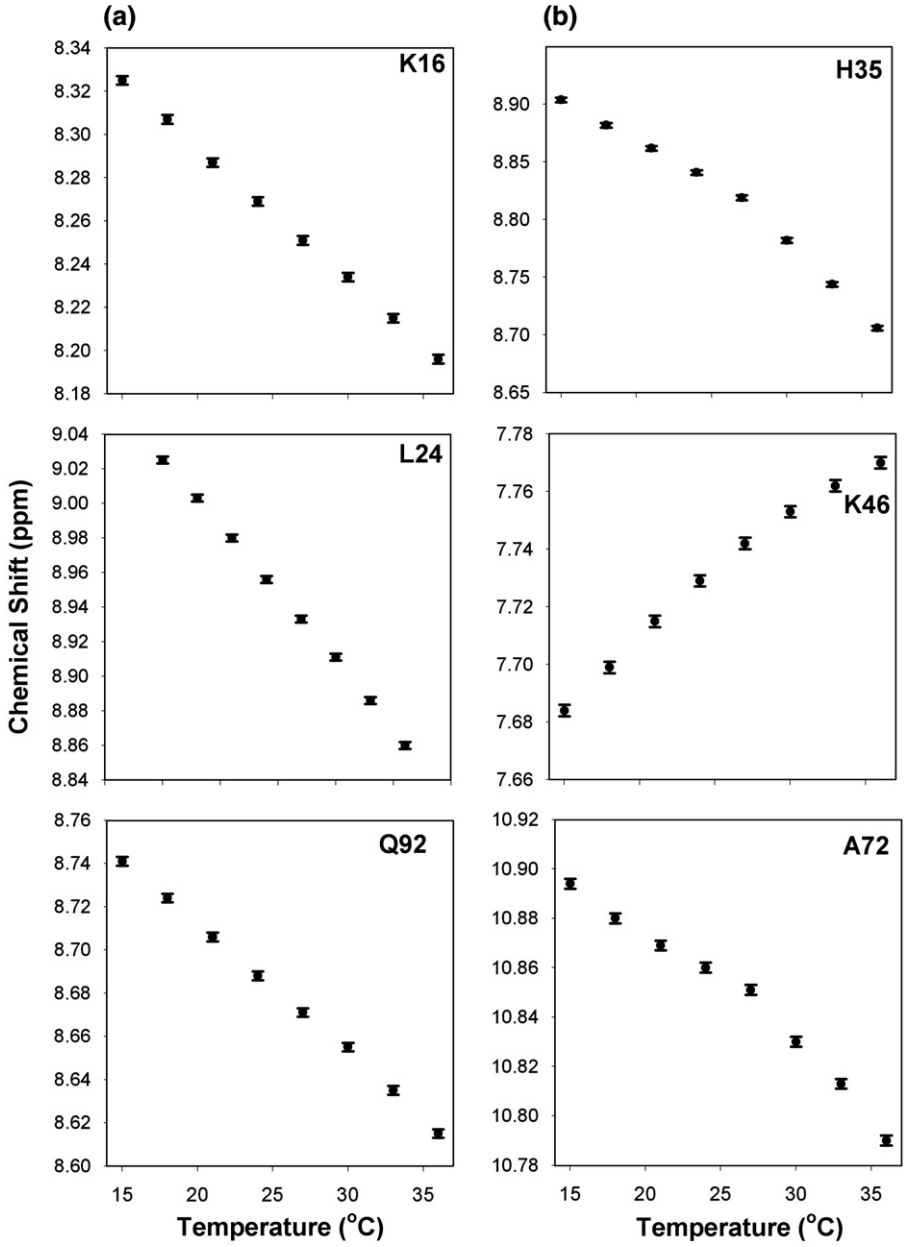

Figure 3. Residues showing linear and non-linear chemical shift variation with temperature for SUMO-1 at pH 5.6. (a) Linear profiles and (b) non-linear profiles.

The peak assignments in the native protein at 300 K, pH 7.4 have already been reported earlier.[25] The HSQC spectrum of SUMO-1 at pH 5.6 was very similar, so most of the peaks were easily identified by visual inspection. However, to remove some ambiguities in crowded regions, we recorded the standard triple resonance experiments (see Materials and Methods) on a doubly (^{13}C, ^{15}N) labeled sample and obtained all the sequence-specific assignments. The HSQC spectrum of SUMO-1 with all the peak assignments at pH 5.6 and 300 K is shown in Figure S1 (A) of Supplementary Data. The peak assignments in the HSQC spectra at pH 5.6 in 0.35, 0.7 and 0.9 M urea could be readily obtained since all these spectra were nearly identical; Supplementary Data Figure S1 (B) shows an overlay of the spectra at 0 and 0.9 M urea. At each of the urea conditions, we could systematically monitor the peak movements as a function of temperature in the range 288–309 K, since the spectra were recorded at every three degree interval. These experiments were repeated three times with freshly prepared samples on different days to check for the reproducibility of the data and the profiles were indeed found to be reproducible.

In the native state of SUMO-1, most of the residues show linear dependence of the chemical shift with temperature, however, some residues do show non-linear dependence and with different profiles. Some of these profiles are shown in Figure 3: Figure 3(a) shows illustrative linear dependences, and Figure 3(b) shows illustrative non-linear behaviors. Some residues show positive temperature gradients as illustrated by K46. Among those that show curvatures, both convex and concave shapes are seen. Eight out of 93 observable amide protons show curvature in the temperature-dependent chemical shift profiles.

We noticed many interesting patterns as the urea concentration was changed from 0 M to 0.9 M. More and more residues showed curved profiles, and also several profiles changed. Some profiles, which were linear at 0 M, showed considerable curvature at 0.9 M and *vice versa*. For a better appreciation of the curvatures, all the chemical shift *versus* temperature data were fitted to a straight line and the residuals

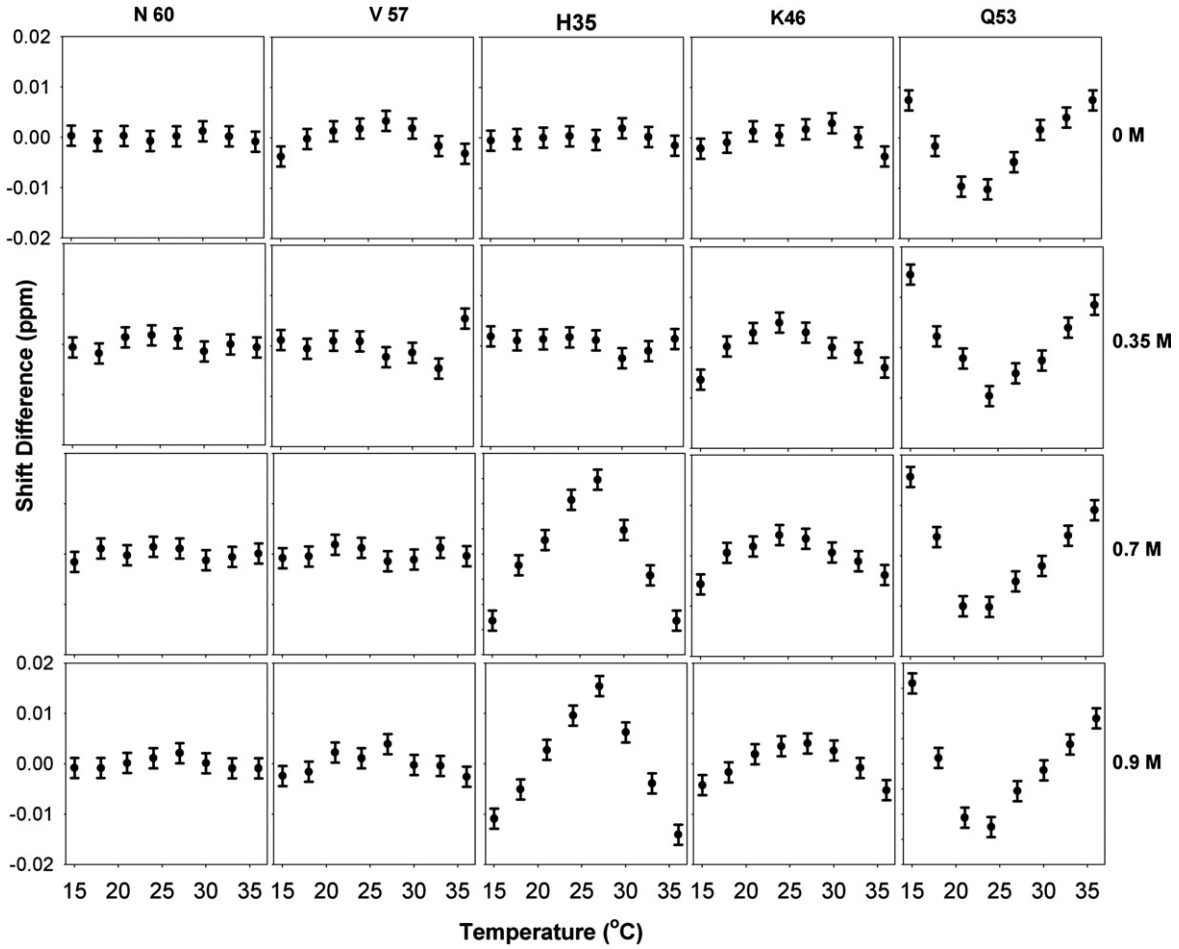

Figure 4. Illustrative examples showing variations in the linear and non-linear profiles of chemical shift variation with temperature. Chemical shifts were fitted to a straight line and the calculated residuals have been plotted against temperature at different urea concentrations. In these plots *y*-axis range was 0.04 ppm, i.e. ±0.02 ppm centered at 0.0 and *x*-axis was 14–37 °C. Error bars indicate chemical shift measurement error, which was ±0.002 ppm. For each row, urea concentration is indicated on the right.

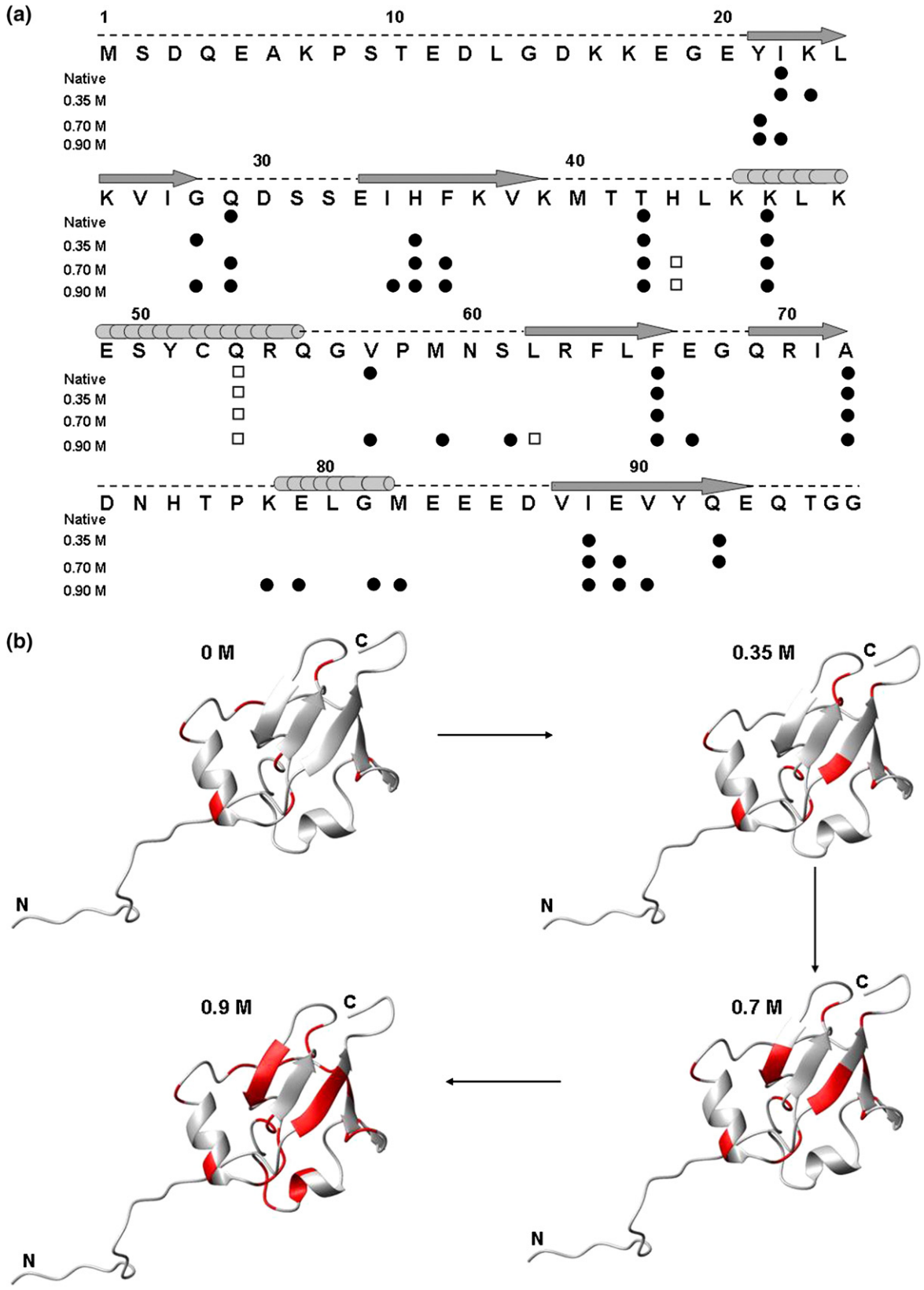

Figure 5. (a) Summary of the non-linear behaviours shown by different residues in SUMO-1 at different urea concentrations. Convex shapes are indicated by filled circles and concave shapes are indicated by open squares. The secondary structure elements in the native structure are shown above the sequence. (b) Residues showing curved temperature dependence at the different urea concentrations are colored in red on the native structure of the protein.

were plotted against temperature as illustrated in Figure 4. Clearly, different residues show different profiles. Many profiles remain linear at all urea concentrations, as seen in the case of N60. Few profiles that are curved at 0 M become linear when the urea concentration is increased, e.g. V57, whereas, in most cases the curvature increases with increase in urea, e.g. H35, K46, Q53. While most of the curvatures are of convex shape some residues depict concave shape, as in Q53. Figure 5(a) shows a summary of the observed different temperature dependence profiles along the sequence of the protein. Figure 5(b) depicts the urea concentration-dependent changes in the number and location of residues accessing alternative conformations on the three-dimensional structure of the protein. We did a similar analysis of the ^{15}N chemical shifts with temperature at all urea concentrations. However, we found ^{15}N to be less sensitive to temperature as compared to amide protons. The deviations from linearity (residuals) were similar or smaller than the errors (~0.02 ppm) in chemical shift measurements (data not shown). Hence, we refrained from an interpretation of these deviations in terms of accessing of the alternative conformations.

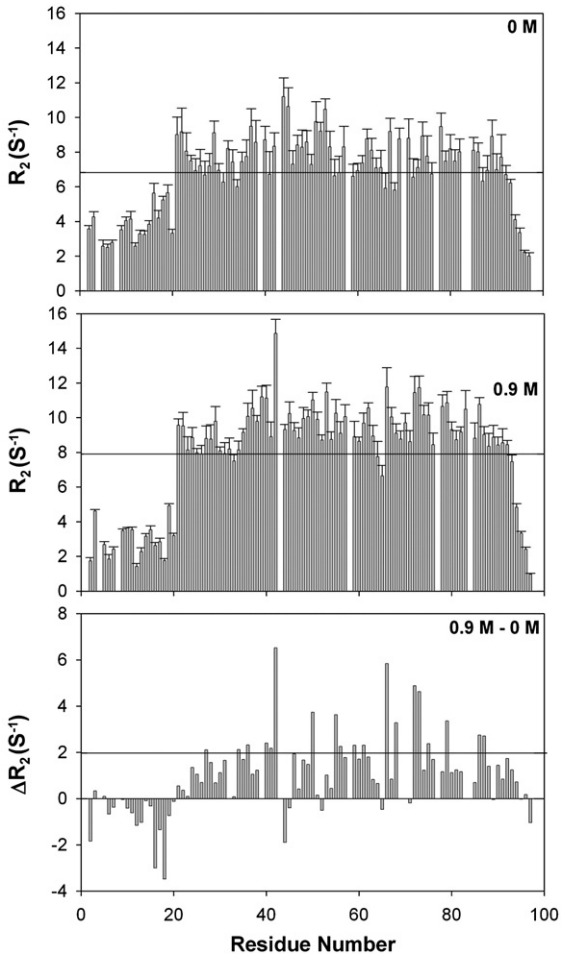

Figure 6. Transverse ^{15}N (R_2) relaxation rates in SUMO-1 under native condition and at 0.9 M urea are plotted against residue number in the top two panels. The error bars are indicated for each residue. The average errors in the top and the middle panels were 0.6 and 0.45 s^{-1}, respectively. The line in each box indicates the average value. The bottom panel shows differences (ΔR_2) in the above transverse relaxation rates. ΔR_2 deviations larger than 2 s^{-1} (which is more than three times the average error (0.6 s^{-1}) in the R_2 values) are taken to indicate enhancement of conformational exchange when urea concentration was increased.

Conformational transitions in SUMO-1 in the native and near-native states

The ^{15}N transverse relaxation rates (R_2) provide valuable indications for the conformational transitions occurring on milliseconds to microseconds time scales. The presence of conformational exchange for a particular residue will contribute to an increase in the transverse relaxation rate (R_2) ($R_2 = R_{2,int+} R_{ex}$ where $R_{2,int}$ is the intrinsic rate and R_{ex} is the contribution due to exchange). We measured the R_2s for SUMO-1 under native condition (0 M urea) and also at 0.9 M urea, and the results are shown in Figure 6. It may be seen that the flexible N terminus becomes even more flexible when the urea concentration is increased, whereas, in the central portion many residues show significant increase in the transverse relaxation rates. These reflect on the changes in the energy landscape of the protein as the urea concentration is increased.

Discussion

Thermal denaturation

The thermal denaturation profile monitored by far-UV CD reveals that SUMO-1 is a very stable protein. It unfolds by a simple co-operative two state process with a T_m of 334.64(±0.08) K. This is in contrast to the denaturant-dependent unfolding, which was found to be complex.[26] It is quite plausible that the two unfolding phenomena populate different denatured states.

For SUMO-1 we obtained higher ΔH and ΔC_p values compared to other proteins of similar size; these data are available in PROTHERM data bank. There seems to be a loose correlation that proteins with low free energies of unfolding and large heat capacities show higher increase in flexibility with temperature.[36] This could have some relevance to many residues showing curvature in temperature-dependent chemical shift changes in the near-native condition of the protein.

Curved temperature dependence of amide proton chemical shifts

As indicated earlier, curvature in temperature dependence of amide proton chemical shift of a particular residue indicates that the residue accesses alternative conformations. Several studies performed by Williamson and co-workers[10–12] have shown that the alternative states thus identified

represent locally unfolded forms, typically consisting of approximately five amino acid residues centered on the residue that displays curved temperature dependence.[10–12] As shown in Figure 5(a), in the native condition of SUMO-1, about eight residues show curvature in temperature-dependent chemical shifts. Upon addition of urea more residues seem to be participating in conformational exchange and thus acquire curved profiles. In the case of 0.35 M and 0.7 M urea concentrations the number of residues showing curvature in temperature-dependent chemical shift profiles are 11 and 13, respectively, which increases to 25 at 0.9 M urea concentration. Comparing the magnitudes of the curvatures with those seen in the simulations for the same temperature range, we can infer that the alternative conformations lie within 2 kcal/mol from the ground state and in some cases where the curvature is very deep the energy may even be less than 1 kcal/mol.

Figure 5(b) shows the progressive changes in the number and location of residues that access alternative conformations. To start with, at 0 M condition, the residues exhibiting curved temperature dependence are located either in the loop or at the edges of the structural elements. As the urea concentration increases, the residues located in the close proximity of these residues attain flexibility. At 0.9 M urea, 25 out of 93 residues exhibit curvature implying that the protein becomes conformationally quite dynamic. Most of these residues are located in the β2, β5 strands, at the edges of the helices, and in the loops surrounding these elements.

Positive temperature gradients

As mentioned before, the temperature coefficient for an amide proton is generally negative and this is a consequence of weakening of H-bond on increasing the temperature. Positive temperature coefficients originate from structural perturbations such as changes in ring currents, or, in general, those perturbations that cause downfield shifts of the amides. In the present case, positive coefficients are seen for the residues K46, L62 and V90 and these residues are located in α1, at the beginning of β3 and in β5, respectively. The possible reason for the positive temperature gradient could be that these residues are upfield shifted from their respective random coil values in the native structure. If we consider the chemical shift of the urea-denatured state as random coil value, then these amides resonate at least 1 ppm upfield compared to their random coil values. As the temperature increases, the local structural perturbation causes a downfield shift of these amides. L62 and V90 have positive gradients with a linear profile while K46 shows a convex curve.

Mechanistic insights into the non-linear profiles

Understanding the possible reason for the conformational flexibility is very crucial for defining the shape of the energy landscape. The eight residues that clearly show curved temperature dependence under the native condition, are: I22, Q29, T42, K46, Q53, V57, F66, and A72. A closer look into the structural arrangement of the side-chains around these residues would provide some clues to the origin of the conformational flexibilities. Figure 7 provides an insight into the behaviors of T42, K46 and A72. The side-chains of residues A72 and T42 are seen to be in close vicinity of H75 and H43 side-chains. Now, as our experiments were performed at pH 5.6, and at this pH the side-chains of histidine residues (H, pK ~6) will be inter-converting between protonated and deprotonated states, there will be fluctuations in the surroundings of the histidine side-chains. These in turn could induce backbone fluctuations. We may mention here that the pH of the solution changes by about 0.07 unit as the temperature increases from 15 to 35 °C in a buffer of pH 6.[37] In the present study, a similar pH change is expected, since the experimental conditions are comparable (pH 5.6 and temperature range, 15–36 °C). However, this small change in pH should not affect the protonation-deprotonation of the histidine side-chains.

Further, in Figure 7 we also see that K46 and T42 are in close proximity to the side-chains of F36. Thus ring flips of F36 can also cause local structural fluctuations including backbone fluctuations. All these effects account for the curved temperature dependences observed for the residues, T42, K46 and A72. Similar arguments would apply for the other five residues as well, though they are not explicitly discussed here. Overall, there could be both backbone fluctuations, and/or side-chain fluctuations that would contribute to curved temperature dependence of amide proton chemical shifts.

Energy landscape of the native state ensemble

Identification of the residues accessing alternative conformations in the native and near-native states created by sub-denaturing concentrations of urea enables characterization of the plasticity of the energy landscape, on one hand, and provides a gross view of the landscape of the native state ensemble on the other. As shown in Figure 4, the curvatures for H35 and K46 increase, whereas that for Q53 remains almost the same. Simulation results from Figure 2 illustrate that the increase in curvature is a reflection on the contraction of the energy landscape, i.e. the ground state and the excited state come closer. In general, the energy landscape of SUMO-1 seems to contract as the urea concentration is increased and the effect of this is reflected by an increase in the number of residues with curved temperature dependence profiles. This is not too surprising since upon interaction urea causes local perturbation in the structural elements and these disturbances will be relayed to the neighboring residues because of side-chain packing. At least 25 out of 93 observable peaks show signatures of

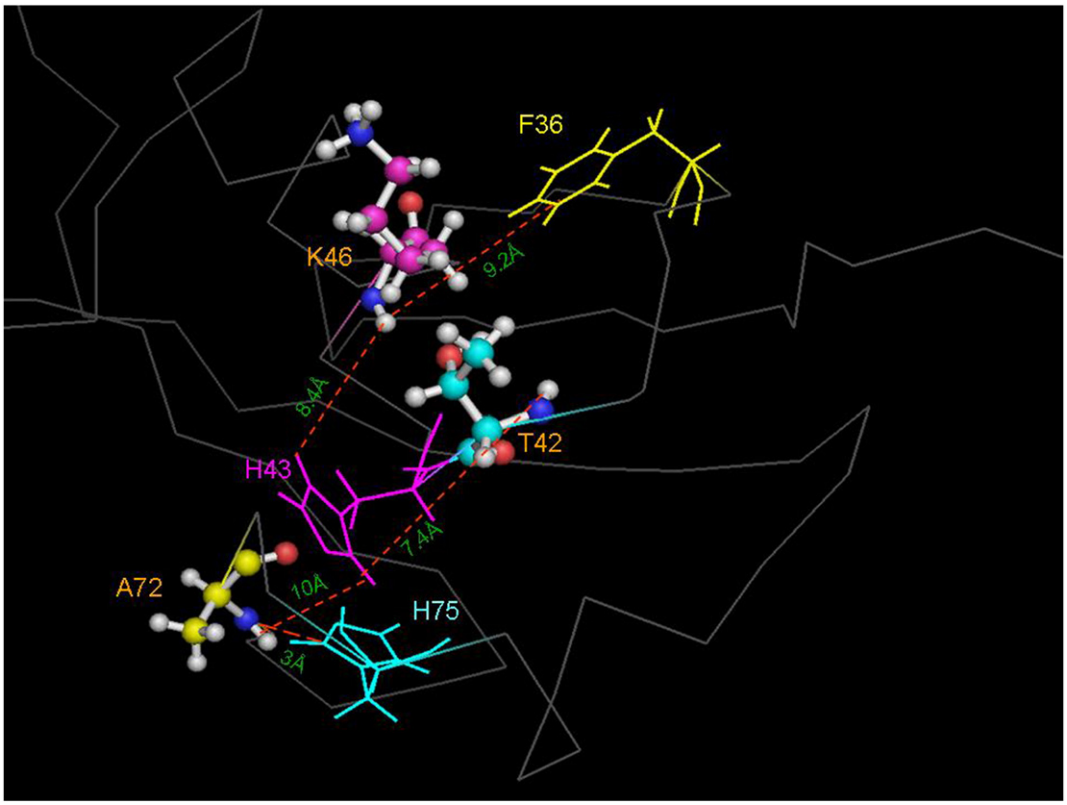

Figure 7. Zoom on a particular portion of the structure of the protein. Topological arrangement of His side-chains and aromatic rings around the residues showing curved temperature dependences. Residues with curved temperature dependence, T42, K46 and A72, are located at ≤10 Å from the His side-chains or aromatic rings.

alternative conformations. Judging from the location of the residues on the protein structure, it is obvious that edges of helices, β2, β5 and loops around them are more vulnerable sites for perturbations.

Further, from the ^{15}N transverse relaxation rates (R_2) (Figure 6), which provide insights into milliseconds to microseconds time scale conformational exchange, we observe sequence-wise variations as the urea concentration is increased from 0 M to 0.9 M. The N-terminal residues that are already flexible attain greater flexibility as evidenced by decrease in R_2. A significant increase in the R_2 can be discerned in the structured part of protein. The residues with $\Delta R_2 > 2\ s^{-1}$ have been identified and mapped on the structure of the protein. The cut-off of $2\ s^{-1}$ was chosen because it was more than three times the average error ($0.6\ s^{-1}$) in the R_2 values. Figure 8 provides an all-inclusive (0, 0.35, 0.7 and 0.9 M urea) comparison of the residues showing curved temperature dependence (a) with those showing $\Delta R_2 > 2\ s^{-1}$ (b). Interestingly, there is a nice correlation between the two.

The alternative states identified by curved temperature dependence of amide proton chemical shifts are within 1–2 kcal/mol from the ground state. These states are in fast exchange with the ground state on the chemical shift time scale because we observed only one peak for each residue. This implies that the exchange rate for the excited state to the native state inter-conversion is at least ~1000 s^{-1}. The activation free energy, ΔG_{act} can be given as: $\Delta G_{act} \cong -RT\ln\vec{k}$ where $\vec{k}$ is the rate constant. The highest possible activation energy for such an exchange rate has been calculated to be ~4 kcal/mol.[38] This implies that there is an energy barrier between the two states and this is about 2–3 kcal/mol above the excited state.

Correlations with target binding sites

SUMO-1 is known to bind to a variety of target proteins with diverse structures. It is therefore imperative that there is an induced adjustment of the structure to acquire maximum specificity of interaction, and the adaptability of the protein structure as can be gauged by the residue-wise accessing of alternative conformations described above would be of great significance. In our previous study we have identified the non-covalent interaction site of SUMO-1 with Dynamin, a protein involved in clathrin-mediated endocytosis.[25] In recent years, it has been shown that the prominent mode of non-covalent interaction by SUMO-1 proceeds by recognition of SUMO binding motifs on the substrate site.[39–41] Figure 8(c) shows the residues that were seen to be perturbed when GED (GTPase effector domain) of Dynamin[25] and SBMs (SUMO binding motifs)[39–41] interacted with SUMO-1. The binding surfaces for these two substrates lie on the opposite faces of the protein. In sumoylation reaction, SUMO-1 covalently attaches to the side-chain of a lysine in the target molecules. This modi-

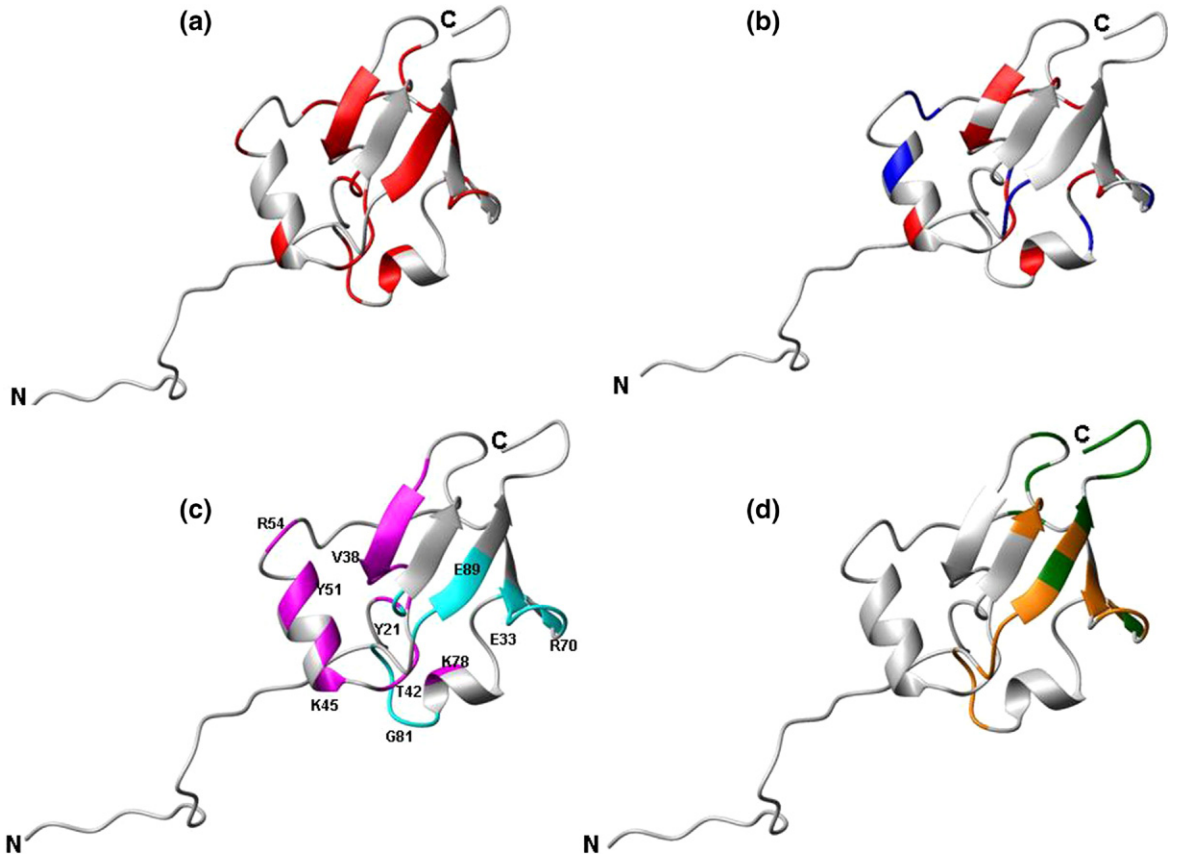

Figure 8. Comparison of residues with curved temperature dependence profile shown in (a) with the residues showing $\Delta R_2 > 2\ s^{-1}$ when urea concentration was increased from 0 M to 0.9 M (b) and the residues involved in substrate binding (c). For (b), all the residues colored in red are showing both the properties, i.e. curved temperature dependence and $\Delta R_2 > 2\ s^{-1}$. The residues in blue are those that have $\Delta R_2 > 2\ s^{-1}$ but do not show curved temperature dependence. In the case of (c) residues of SUMO-1 engaged in non-covalent interaction with GED (cyan) and with SBMs (pink) are indicated on the three-dimensional structure of the protein. Some residues are labeled to judge the locations. (d) The residues of SUMO-1 involved in interaction with E1 (dark green) and with E2 (orange) enzymes are highlighted.

fication is mediated by cascade of three enzymes, namely E1 (activating enzyme), E2 (conjugating enzyme) and ligating enzymes (E3). The crystal structure of SUMO-1 in complex with E1 enzyme (SAE1/2) has been solved recently. The authors have shown that the substrate E1 (SAE1/2) recognition site lies near and around the C terminus of SUMO-1.[42] The site where SUMO-1 binds with its E2 (UBC9) has also been identified by NMR chemical shift perturbations.[43] Figure 8(d) summarizes the results of these interactions with SUMO-1 in color-coded manner on the protein surface. Interestingly, there is a close match between the residues that are perturbed on protein binding and those that were seen to be accessing alternative conformations in the present study.

In a recent similar study using variable pressure NMR spectroscopy on ubiqutin and NEDD8 it has been shown that the two proteins exhibit conformational fluctuation in the evolutionarily conserved enzyme-binding sites.[44] These proteins also have a structurally similar locally disordered conformer in equilibrium with the native folded conformer. Thus they seem to have similar structures not only in their basic folded states, but also in their high-energy states. The authors showed that the structure of the protein in these excited states is similar to the structure of the protein in the complex with their activating enzymes. Thus, these high energy conformers are suggested to be the functional forms of the protein. SUMO-1, a UBL (ubiquitin-like protein), is similar to these two proteins in many respects: they have the same three-dimensional fold, the mechanisms by which they get ligated to the substrates are also similar. It is quite exciting to note that our findings provide similar insight into the details of SUMO-1 binding to its substrate.

Conclusions

We have attempted here to obtain a residue level view of the energy landscape of the native state ensemble of SUMO-1. Curvature in temperature dependence of amide proton chemical shifts provided a useful insight into the rapid accessing of alternative conformations by the individual residues in the protein structure. The data enabled identifica-

tion of residue level changes in the energy landscape due to addition of small concentrations of urea, the protein still remaining entirely in the native state ensemble. In the native state of the protein, only eight residues show curved temperature dependence and this number increases as small amount of urea is added to it. At 0.9 M almost 27% of residues spread over the length of the chain attain conformational flexibilities. These occur at particular regions on the protein structure, namely, edges of the helices, β2, β5 strands and the loops connecting the different structured elements. We also observed that while a large number of residues displayed the typical linear temperature dependence with negative coefficients, some residues displayed positive temperature coefficients. These also reflect on some local structural perturbations other than simple H-bond disturbances. The alternative states accessed by the various residues are within 1–2 kcal/mol from the ground state. The transverse relaxation rates indicate occurrence of slow conformational transitions for many residues and this concurs largely with the accessing of alternative conformations by the different residues. These will have great significance for the adaptability of the protein structure due to external perturbations and thus are functionally very significant. We actually observed a close correlation between the sites accessing alternative conformations and the sites involved in binding to different substrates, like E1 and E2 enzymes of sumoyalation machinery, GED, and SBMs.

Materials and Methods

Protein preparation

SUMO-1 was prepared and purified as described elsewhere.[25] The purity of the protein sample was confirmed by SDS-PAGE.

NMR samples

For NMR studies ^{15}N and (^{15}N, ^{13}C) labeled protein samples were concentrated to ~1.0 mM in an ultrafiltration cell using a 3 kDa cutoff membrane. Protein was exchanged with phosphate buffer (pH 5.6) (100 mM phosphate, 150 mM NaCl, 5 mM EDTA, 1 mM DTT). The final volumes of the samples were ~550 μl (90% H_2O + 10% ^2H_2O).

NMR data acquisition and processing

All the NMR experiments were recorded using a triple channel Varian Inova 600 MHz NMR spectrometer equipped with pulse-shaping and pulse field gradient capabilities. For all the experiments ^1H and ^{15}N and ^{13}C carrier frequencies were set at water (4.74), 116.63 and 56 ppm, respectively. The proton chemical shifts were referenced using DSS as external calibration agent at 0.00 ppm whereas ^{15}N and ^{13}C was referenced indirectly as described by Wishart *et al.*[45] For resonance assignment, several 3D experiments (reviewed by Tugarinov *et al.*[46]), namely, HNCA, HN(CO)CA, ^{15}N-edited TOCSY, C(CO)NH, and HC(CO)NH were performed. For the HNCA spectrum the delay T_N was set to 25 ms. A totalof 64 and 43 complex points were used along t_2 (^{13}C) and t_1 (^{15}N) dimensions, respectively. The HN(CO)CA spectrum was recorded with the same T_N parameter, the same number of t_2 and t_1 points, and the T_{CC} delay was set to 9 ms. C(CO)NH and HC(CO)NH were performed with 64 and 43 complex points, respectively, along the t_2 (^{13}C) and t_1 (^{15}N) dimensions. For the ^{15}N-edited TOCSY-HSQC the mixing time was 80 ms. A total of 80 and 43 increments were used along the indirect ^1H (t_2) and ^{15}N (t_1) dimensions, respectively. In every case 1024 complex data points were collected along t_3. Temperature coefficients of the backbone amide protons in SUMO-1 in 0, 0.35, 0.7 and 0.9 M urea were determined by recording eight ^1H-^{15}N HSQC spectra in each case with 2048 data points and 256 t_1 increments in the temperature range, 15–36 °C, at 3 deg. C intervals. Temperature calibration was done using glycerol. All the data were processed using FELIX on a Silicon Graphic, Inc. work station. Prior to Fourier transformation and zero-filling, data were apodized with a sine-squared weighting function shifted by 60° in both dimensions. After zero filling and Fourier transformation the final matrix had 4096 and 1024 points along F_2 and F_1 dimensions, respectively, for all the HSQC experiments. The chemical shift assignment was done using peak picking macro of FELIX. The chemical shift data were then analyzed by linear regression to estimate the slope and hence the residuals (deviation of the experimental values from the expected values). ^{15}N transverse relaxation rates (R_2) were measured using CPMG delays, 10, 50, 70*, 90, 130, 170*, 210, 250 ms, where asterisks indicates duplicate measurements required for error analysis. Pre-scan delay was 1 s. The rates were extracted from single exponential fits using the Sigma Plot 8.0 software.

CD measurements

Far-UV circular dichroism (CD) at 222 nm was used to monitor the thermal unfolding of SUMO-1, on a JASCO–J810 spectropolarimeter, using 1 nm bandwidth for the measurements. Experiments were performed with 80 μM protein using quartz cuvette of 0.2 cm path length placed on a thermostatted cell holder attached with a thermometer. Data were collected at pH 5.6 in phosphate buffer using automated experiment manager application of JASCO software. The temperature was raised from 10 °C to 80 °C with heating rate of 0.5 deg.C/min, monitoring ellipticity at 222 nm. At every 2 deg.C interval, samples were equilibrated for 10 min and a spectrum from 260 nm to 210 nm was collected. At the end of the heating experiment, the sample temperature was returned to 10 °C with the same rate as during heating to check the extent of reversibility.

CD data analysis

The thermal denaturation data obtained from experiment was smoothened using three points averaging. Thermal unfolding of SUMO-1 showed a two-state ($N \Leftrightarrow U$) sigmoidal behaviour. At each temperature, T, the unfolded fraction (f_{app}) was calculated using equation (3):

$$f_{app} = \frac{S_{obs} - S_0}{S_F - S_0} \quad (3)$$

where, f_{app} is the relative CD signal that shows the apparent unfolded fraction, S_0, S_{obs} and S_F represent the CD signal for the completely folded state, at a particular temperature, and for the thermally unfolded state, respectively. The apparent equilibrium constant of unfolding ($K_{T(app)}$) and the corresponding free energy change (ΔG^0_T) at temperature, T were calculated using equations (4) and (5), respectively:

$$K_{T(app)} = \frac{f_{app}}{1 - f_{app}} \quad (4)$$

$$\Delta G^0_T = -RT \ln(K_{T(app)}) \quad (5)$$

where R is the gas constant and T is the absolute temperature. The associated changes in enthalpy (ΔH_T) and entropy (ΔS_T) were calculated at temperature T, as follows:

$$\Delta G^0_T = \Delta H_T - T\Delta S_T \quad (6)$$

If we assume that heat capacity change (ΔC_p) between native state and denatured state is independent of the temperature in the range of experimental conditions, then ΔH_T and ΔS_T can be written as:

$$\Delta H_T = \Delta H_m + \Delta C_P(T - T_m) \quad (7)$$

$$\Delta S_T = \Delta S_m + \Delta C_p \ln\left(\frac{T}{T_m}\right) \quad (8)$$

where ΔH_m and ΔS_m are the enthalpy and entropy changes, respectively, at the transition mid point (T_m). So at temperature T_m, K_{app} will be 1 and thus $\Delta G^0_m = 0$.

So equation (6) can be rewritten as:

$$\Delta G^0_T = \Delta H_m\left(1 - \frac{T}{T_m}\right) + \Delta C_p\left(T - T_m - T \ln\frac{T}{T_m}\right) \quad (9)$$

Acknowledgements

We thank Dr Rohit Mittal and Dr Ram Kumar Mishra (Department of Biological Sciences, TIFR) for providing the plasmid of SUMO-1, and the Government of India for providing financial support to the National Facility for High Field NMR at the Tata Institute of Fundamental Research.

Supplementary Data

Supplementary data associated with this article can be found, in the online version, at doi:10.1016/j.jmb.2007.01.035

References

1. Kay, L. E. (2005). NMR studies of protein structure and dynamics. *J. Magn. Reson.* **173**, 193–207.
2. Mittermaier, A. & Kay, L. E. (2006). New tools provide new insights in NMR studies of protein dynamics. *Science*, **312**, 224–228.
3. Kumar, S., Ma, B., Tsai, C. J., Sinha, N. & Nussinov, R. (2000). Folding and binding cascades: dynamic landscapes and population shifts. *Protein Sci.* **9**, 10–19.
4. Boehr, D. D., McElheny, D., Dyson, H. J. & Wright, P. E. (2006). The dynamic energy landscape of dihydrofolate reductase catalysis. *Science*, **313**, 1638–1642.
5. Lassalle, M. W. & Akasaka, K. (2007). The use of high-pressure nuclear magnetic resonance to study protein folding. *Methods Mol. Biol.* **350**, 21–38.
6. Kitahara, R., Yokoyama, S. & Akasaka, K. (2005). NMR snapshots of a fluctuating protein structure: ubiquitin at 30 bar-3 kbar. *J. Mol. Biol.* **347**, 277–285.
7. Kamatari, Y. O., Kitahara, R., Yamada, H., Yokoyama, S. & Akasaka, K. (2004). High-pressure NMR spectroscopy for characterizing folding intermediates and denatured states of proteins. *Methods*, **34**, 133–143.
8. Li, H. & Akasaka, K. (2006). Conformational fluctuations of proteins revealed by variable pressure NMR. *Biochim. Biophys. Acta*, **1764**, 331–345.
9. Baxter, N. J. & Williamson, M. P. (1997). Temperature dependence of ^{1}H chemical shifts in proteins. *J. Biomol. NMR*, **9**, 359–369.
10. Baxter, N. J., Hosszu, L. L., Waltho, J. P. & Williamson, M. P. (1998). Characterisation of low free-energy excited states of folded proteins. *J. Mol. Biol.* **284**, 1625–1639.
11. Tunnicliffe, R. B., Waby, J. L., Williams, R. J. & Williamson, M. P. (2005). An experimental investigation of conformational fluctuations in proteins G and L. *Structure (Camb.)*, **13**, 1677–1684.
12. Williamson, M. P. (2003). Many residues in cytochrome c populate alternative states under equilibrium conditions. *Proteins: Struct. Funct. Genet.* **53**, 731–739.
13. Johnson, E. S. (2004). Protein modification by SUMO. *Annu. Rev. Biochem.* **73**, 355–382.
14. Melchior, F., Schergaut, M. & Pichler, A. (2003). SUMO: ligases, isopeptidases and nuclear pores. *Trends Biochem. Sci.* **28**, 612–618.
15. Arcon-Vargas, D. & Ronai, Z. (2002). SUMO in cancer–wrestlers wanted. *Cancer Biol. Ther.* **1**, 237–242.
16. Seeler, J. S. & Dejean, A. (2001). SUMO: of branched proteins and nuclear bodies. *Oncogene*, **20**, 7243–7249.
17. Verger, A., Perdomo, J. & Crossley, M. (2003). Modification with SUMO. A role in transcriptional regulation. *EMBO Rep.* **4**, 137–142.
18. Steffan, J. S., Agrawal, N., Pallos, J., Rockabrand, E., Trotman, L. C., Slepko, N. *et al.* (2004). SUMO modification of Huntingtin and Huntington's disease pathology. *Science*, **304**, 100–104.
19. Gill, G. (2004). SUMO and ubiquitin in the nucleus: different functions, similar mechanisms? *Genes Dev.* **18**, 2046–2059.
20. Girdwood, D. W., Tatham, M. H. & Hay, R. T. (2004). SUMO and transcriptional regulation. *Semin. Cell Dev. Biol.* **15**, 201–210.
21. Muller, S., Ledl, A. & Schmidt, D. (2004). SUMO: a regulator of gene expression and genome integrity. *Oncogene*, **23**, 1998–2008.
22. Um, J. W. & Chung, K. C. (2006). Functional modulation of parkin through physical interaction with SUMO-1. *J. Neurosci. Res.* **84**, 1543–1554.
23. Bayer, P., Arndt, A., Metzger, S., Mahajan, R., Melchior, F., Jaenicke, R. & Becker, J. (1998). Structure determination of the small ubiquitin-related modifier SUMO-1. *J. Mol. Biol.* **280**, 275–286.
24. Jin, C., Shiyanova, T., Shen, Z. & Liao, X. (2001). Heteronuclear nuclear magnetic resonance assignments, structure and dynamics of SUMO-1, a human

ubiquitin-like protein. *Int. J. Biol. Macromol.* **28**, 227–234.
25. Mishra, R. K., Jatiani, S. S., Kumar, A., Simhadri, V. R., Hosur, R. V. & Mittal, R. (2004). Dynamin interacts with members of the sumoylation machinery. *J. Biol. Chem.* **279**, 31445–31454.
26. Kumar, A., Srivastava, S., Kumar, M. R., Mittal, R. & Hosur, R. V. (2006). Residue-level NMR view of the urea-driven equilibrium folding transition of SUMO-1 (1–97): native preferences do not increase monotonously. *J. Mol. Biol.* **361**, 180–194.
27. Anderson, N. H., Neidigh, J. W., Harris, S. M., Lee, G. M., Liu, Z. & Tong, H. (1997). Extracting information from the temperature gradients of polypeptide HN chemical shifts. 1. The importance of conformational averaging. *J. Am. Chem. Soc.* **119**, 8547–8561.
28. Cierpicki, T. & Otlewski, J. (2001). Amide proton temperature coefficients as hydrogen bond indicators in proteins. *J. Biomol. NMR*, **21**, 249–261.
29. Cordier, F. & Grzesiek, S. (2002). Temperature-dependence of protein hydrogen bond properties as studied by high-resolution NMR. *J. Mol. Biol.* **317**, 739–752.
30. Daley, M. E., Graether, S. P. & Sykes, B. D. (2004). Hydrogen bonding on the ice-binding face of a beta-helical antifreeze protein indicated by amide proton NMR chemical shifts. *Biochemistry*, **43**, 13012–13017.
31. Dyson, H. J., Rance, M., Houghten, R. A., Lerner, R. A. & Wright, P. E. (1988). Folding of immunogenic peptide fragments of proteins in water solution. I. Sequence requirements for the formation of a reverse turn. *J. Mol. Biol.* **201**, 161–200.
32. Ohnishi, M. & Urry, D. W. (1969). Temperature dependence of amide proton chemical shifts: the secondary structures of gramicidin S and valinomycin. *Biochem. Biophys. Res. Commun.* **36**, 194–202.
33. Wagner, G., Pardi, A. & Wuthrich, K. (1983). Hydrogen bond length and ^{1}H NMR chemical shifts in proteins. *J. Am. Chem. Soc.* **105**, 5948–5949.
34. Tilton, R. F., Jr, Dewan, J. C. & Petsko, G. A. (1992). Effects of temperature on protein structure and dynamics: X-ray crystallographic studies of the protein ribonuclease-A at nine different temperatures from 98 to 320 K. *Biochemistry*, **31**, 2469–2481.
35. Cierpicki, T., Zhukov, I., Byrd, R. A. & Otlewski, J. (2002). Hydrogen bonds in human ubiquitin reflected in temperature coefficients of amide protons. *J. Magn. Reson.* **157**, 178–180.
36. Seewald, M. J., Pichumani, K., Stowell, C., Tibbals, B. V., Regan, L. & Stone, M. J. (2000). The role of backbone conformational heat capacity in protein stability: temperature dependent dynamics of the B1 domain of Streptococcal protein G. *Protein Sci.* **9**, 1177–1193.
37. Fukuda, H. & Takahashi, K. (1998). Enthalpy and heat capacity changes for the proton dissociation of various buffer components. *Proteins: Struct. Funct. Genet.* **33**, 159–166.
38. Kubelka, J., Hofrichter, J. & Eaton, W. A. (2004). The protein folding 'speed limit'. *Curr. Opin. Struct. Biol.* **14**, 76–88.
39. Hecker, C. M., Rabiller, M., Haglund, K., Bayer, P. & Dikic, I. (2006). Specification of SUMO1- and SUMO2-interacting motifs. *J. Biol. Chem.* **281**, 16117–16127.
40. Song, J., Durrin, L. K., Wilkinson, T. A., Krontiris, T. G. & Chen, Y. (2004). Identification of a SUMO-binding motif that recognizes SUMO-modified proteins. *Proc. Natl Acad. Sci. USA*, **101**, 14373–14378.
41. Song, J., Zhang, Z., Hu, W. & Chen, Y. (2005). Small ubiquitin-like modifier (SUMO) recognition of a SUMO binding motif: a reversal of the bound orientation. *J. Biol. Chem.* **280**, 40122–40129.
42. Lois, L. M. & Lima, C. D. (2005). Structures of the SUMO E1 provide mechanistic insights into SUMO activation and E2 recruitment to E1. *EMBO J.* **24**, 439–451.
43. Liu, Q., Jin, C., Liao, X., Shen, Z., Chem, D. J. & Chen, Y. (1999). The binding interface between an E2 (UBC9) and a ubiquitin homologure (UBL1). *J. Biol. Chem.* **274**, 16979–16987.
44. Kitahara, R., Yamaguchi, Y., Sakata, E., Kasuya, T., Tanaka, K., Kato, K. *et al.* (2006). Evolutionally conserved intermediates between ubiquitin and NEDD8. *J. Mol. Biol.* **363**, 395–404.
45. Wishart, D. S., Bigam, C. G., Yao, J., Abildgaard, F., Dyson, H. J., Oldfield, E. *et al.* (1995). ^{1}H, ^{13}C and ^{15}N chemical shift referencing in biomolecular NMR. *J. Biomol. NMR*, **6**, 135–140.
46. Tugarinov, V., Hwang, P. M. & Kay, L. E. (2004). Nuclear magnetic resonance spectroscopy of high-molecular-weight proteins. *Annu. Rev. Biochem.* **73**, 107–146.

Edited by P. Wright

(Received 18 December 2006; received in revised form 11 January 2007; accepted 12 January 2007)
Available online 20 January 2007